in the atomic calculations. One might expect then that, in two molecules which differ only in the substitution of B for A, the localized orbitals of the rest of the molecule containing A could be used to calculate the corresponding molecular matrix element with an error of the order of magnitude of 5%; *i.e.*, the 50% error in the atomic case is weighted by the contributions of the A and B atomic core regions to the localized orbital. Thus, although atomic transferability as tested in this paper is shown not to be an accurate method for approximating atomic orbitals, localized orbitals may be transferable to a useful accuracy; but that can be demonstrated only by direct calculation.

If one assumes that localized orbitals for some kinds of molecules will be transferable to a useful degree of accuracy, one is led to consider the physical consequences of the transferability. For example, one should consider the possibility that the potential surfaces of these molecules may be interrelated except for core contributions. To be more specific, if the H^- orbital is transferable in the case of LiH and NaH, one might expect that the potential curves of each at identical nuclear separations will differ primarily due to the differences between the Li^+ and Na^+ ions, differences which should become pronounced only as the hydrogen nucleus penetrates into the Li and Na core regions. If this is the case, can the corrections be introduced without resort to full electronic calculations? Clearly these are not the only speculations one can make if one assumes that there are transferable localized orbitals; but it is also clear that the next step needed is molecular transferability calculations, not extensive speculations.

Conclusions

One general conclusion to be drawn from this study is that *ab initio* Hartree–Fock valence atomic orbitals have properties consistent with the idea of chemical periodicity. This is a very interesting result since these orbitals contain no adjustable parameters on which one might build in the periodicity. The periodicity is a consequence of the quantum mechanical equations. Some implications of this have been discussed. In addition to this general conclusion, the following specific conclusions may be drawn from the calculations.

The atomic valence-shell Hartree–Fock orbitals of congeners are generally about the same size and in some cases are nearly identical except in the atomic core region. The differences in the core region when two valence orbitals are nearly identical outside of the core seem to be due primarily to the valence orbitals being orthogonal to different core orbitals. The accuracy to which the valence-shell orbitals of one atom approximate those of another depends upon the energies of the valence orbitals of each symmetry being nearly equal for the two atoms. This means that the valence-shell orbitals of two atoms may be nearly identical even though they are not congeners. The use of the valence-shell orbitals of one atom as approximations to the valence-shell orbitals of another atom is not justified in the calculation of most energy integrals. The Slater two-electron integrals can be approximated in this way with errors of less than 10% for transfers of valence orbitals from third- to fourth-period congeners in columns III through VI.

Acknowledgments. I thank Dr. P. S. Bagus for helping me to find the last error in my program and for giving me his atomic Hartree–Fock orbitals before publication, and Mr. E. R. Raas for teaching me to run Rutgers' IBM 7040. In addition I am grateful to many friends at the Pennsylvania State University for their advice on how to speed up a computer program.

Theoretical Band Shapes for Vibronically Induced Electronic Transitions

Lawrence L. Lohr, Jr.

Contribution from the Department of Chemistry, University of Michigan, Ann Arbor, Michigan. *Received September 15, 1969*

Abstract: Intensity distributions associated with vibronically induced electronic transitions are calculated by a method in which the vibrational wave functions of both the initial and final electronic states are expanded in a truncated basis of harmonic oscillator eigenstates. Results are given for transitions between harmonic oscillators with different force constants, between harmonic oscillators with different equilibrium positions, and between a harmonic oscillator and a double-minimum well. The distributions are characterized by their spectral moments and by bar-graph plots of the spectra. Comparisons are made to the corresponding Franck–Condon distributions for an allowed transition, showing differences that might serve as evidence for a vibronic intensity mechanism in an experimental spectrum.

In the analysis of absorption band shapes of electronic transitions thought to be vibronically induced a simplifying assumption is often made, namely that the intensity distribution with respect to the vibronically active mode consists at 0°K of but a single line, this $0 \rightarrow 1$ transition being in effect a false origin upon which are built normal Franck–Condon distributions with respect to the remaining modes, including the totally symmetric vibration. At higher temperatures there would be two origins, corresponding to $\Delta v = \pm 1$, where

v is the quantum number associated with the vibronically active mode. This simplification assumes that this mode is simply a harmonic oscillator with no change in either force constant or equilibrium geometry upon changing electronic states. We recently noted[1] that changes in force constant or geometry did not affect the temperature dependence of the total vibronically induced oscillator strength f since the familiar form

$$f(T) = f(0°\mathrm{K}) \coth (h\nu/2kT) \tag{1}$$

depends only on assuming a harmonic oscillator of frequency ν for the initial electronic state. More generally $f(T)/f(0)$ is completely determined by the form of the potential curves in the initial electronic state, this state being the ground state in absorption or an excited state in emission that is Boltzmann-equilibrated with respect to vibrations. However, the distribution of intensity will depend upon potential curves for both initial and final states. This distribution is determined not by overlap integrals as with usual Franck–Condon factors but instead by matrix elements of the nuclear coordinate x

$$f_{ij}(T) = A|\langle i|x|j\rangle|^2 P_i(T) \tag{2}$$

where i denotes the ith vibrational level, with a Boltzmann population $P_i(T)$, of the initial electronic state, j denotes the jth level of the final state, A is a constant containing electronic factors, and $f_{ij}(T)$ is the oscillator strength for the transition $i \rightarrow j$. It is assumed[2] that the vibronically induced transition moment is directly proportional to the coordinate x, where x is measured from the equilibrium position in the initial state. We desire to compute theoretical distributions (band shapes) in order to see if there are features that might serve to indicate the presence of vibronically induced transitions in an experimental spectrum.

Method

In order to calculate the intensities of the individual lines, eq 2, and the corresponding shapes it is necessary to know two sets of vibrational energies and wave functions, the sets $\{E_i, \psi_i\}$ and $\{E_j, \psi_j\}$ corresponding to the potential curves for the vibronically active coordinate in the initial and final states, respectively. The method chosen was the expansion of each wave function in a truncated basis of harmonic oscillator (HO) eigenstates. This method is particularly practical when a potential function can be expressed as a power series

$$V(x) = \sum_{n=0} B_n x^n \tag{3}$$

since matrix elements of such a potential with $n \leq 6$ have been reported[3,4] for a HO basis set. In fact this method has been used in studies of asymmetric potentials for hydrogen bonds[5] and of ring deformations in bromocyclobutane and related compounds.[6] We expand both the sets $\{\psi_i\}$ and $\{\psi_j\}$ in the same basis $\{\phi_v\}$

$$\psi_i = \sum_{v=0}^{v_{max}} C_{vi}\phi_v$$
$$\psi_j = \sum_{v=0}^{v_{max}} C_{vj}\phi_v \tag{4}$$

where v is the usual HO quantum number, and the chosen number m of HO basis functions is $v_{max} + 1$.

The eigenvectors C_i and dimensionless eigenvalues E_i' are obtained by diagonalizing an mxm matrix corresponding to the dimensionless Schrödinger equation[5]

$$\frac{-\mathrm{d}^2\psi}{\mathrm{d}\xi^2} + (1/2)V'(\xi)\psi = (1/2)E'\psi \tag{5}$$

which is obtained from

$$\frac{-\hbar^2}{2M}\frac{\mathrm{d}^2\psi}{\mathrm{d}x^2} + V(x)\psi = E\psi \tag{6}$$

by the substitutions[5] $V = (\hbar\beta/4)V'$, $E = (\hbar\beta/4)E'$, and $x = (\hbar/M\beta)^{1/2}\xi$, where β is an arbitrary circular frequency, M is the reduced mass, and ξ is a dimensionless coordinate. Corresponding to eq 3

$$V(\xi) = (\hbar\beta/2)\sum_n b_n\xi^n \tag{7}$$

where

$$b_n = (2/\hbar\beta)(\hbar/M\beta)^{n/2}B_n \tag{8}$$

so that $V'(\xi)$ is simply $2\Sigma_n b_n\xi_n$. Thus the HO defined by $b_2 = 1$, giving $V'(\xi) = 2\xi^2$, has energy spacings of four units of $\hbar\beta/4$ and a zero-point energy (ZPE) of two units. After the matrix diagonalization the eigenvalues are for convenience divided by 2 so that they are in units of $\hbar\beta/2$ rather than $\hbar\beta/4$. Then the ZPE for the basis oscillator becomes one unit of $\hbar\beta/2$. All thermal energies are expressed in this same unit, so that $T = 2$ means that $kT =$ two units of $\hbar\beta/2$, or that $kT/\hbar$ equals the fundamental frequency β of the basis set. The eigenvectors corresponding to this HO serve as basis functions for all other potential energy choices, with each choice defined by a set $\{b_n\}$ with $n \leq 6$.

A computer program was written to set up and diagonalize the matrices corresponding to the potential curves for initial and final electronic states. The necessary kinetic energy matrix elements were also available[3] for our basis set. Then based on eq 4, the program calculates the overlap integrals

$$\langle i|j\rangle = \sum_{v=0}^{v_{max}} C_{vi}C_{vj} \tag{9}$$

and the transition moments

$$\langle i|\xi|j\rangle = \sum_{v=1}^{v_{max}} \langle v|\xi|v-1\rangle[C_{vi}C_{v-1,j} + C_{v-1,i}C_{vj}] \tag{10}$$

where $\langle v|\xi|v-1\rangle = (v/2)^{1/2}$.

A dimensionless energy distribution function $F(E',T)$ can be characterized in terms of spectral semiinvariants[7,8] $\Lambda_k(T)$, defined for our discontinuous distribution as follows

$$\Lambda_1(T) \equiv \overline{E'} = \left[\sum_{i,j} f_{ij}'(T)\Delta E_{ij}'\right]/f'(T) \tag{11a}$$

(1) L. L. Lohr, Jr., *J. Chem. Phys.*, **50**, 4596 (1969).
(2) A. C. Albrecht, *ibid.*, **33**, 156 (1960); also see footnote 5 of ref 1.
(3) E. Heilbronner, Hs. H. Günthard, and R. Gerdil, *Helv. Chim. Acta*, **39**, 1171 (1956).
(4) For a correction to one of the matrix elements in ref 3, see T. Ueda and T. Shimanouchi, *J. Chem. Phys.*, **47**, 4042 (1967).
(5) R. L. Somorjai and D. F. Hornig, *ibid.*, **36**, 1980 (1962).
(6) W. G. Rothschild, *ibid.*, **45**, 1214 (1966).
(7) R. Kubo and Y. Toyosawa, *Progr. Theor. Phys.* (Kyoto), **13**, 160 (1955).
(8) N. S. Hush, *Progr. Inorg. Chem.*, **8**, 391 (1967).

while for $k \neq 1$

$$\Lambda_k(T) \equiv \overline{(E' - \bar{E}')^k} = \{\sum_{i,j} f_{ij}'(T)[\Delta E_{ij}' - \Lambda_1]^k\}/f'(T) \quad (11b)$$

where $f_{ij}'(T)$ corresponds to eq 2, but with ξ replacing x, $\Delta E_{ij}' \equiv E_j' - E_i'$, and $f'(T) \equiv \Sigma(i,j)f_{ij}'(T)$. By contrast, Λ_k corresponding to a Franck–Condon distribution would have $f_{ij}'(T)$ factors obtained from matrix elements in eq 9 rather than eq 10, while the denominator in eq 11 would be temperature independent and equal to unity. The program is written to compute Λ_k for $k = 1$–6, both for allowed and forbidden (vibronically allowed) electronic transitions.

Note that the Λ_k's differ from moments μ_k defined by

$$\mu_k \equiv \overline{(E')^k} = \sum_{i,j} f_{ij}'(T)(\Delta E_{ij}')^k/f'(T) \quad (12)$$

For example, $\Lambda_1 = \mu_1$, but $\Lambda_2 = \mu_2 - \mu_1^2$. The two types of quantities are identical if $\mu_1 = 0$, but since μ_1 (or Λ_1) is in general a function of T, it is better to describe a band shape in terms of the semiinvarients Λ_k rather than μ_k. We shall use the term "moments" in the remainder of this paper to mean the quantities Λ_k. Now Λ_1 is the mean transition energy, which is simply the vibrational energy change if the electronic energy difference is arbitrarily chosen to be zero. The second moment, Λ_2, is related to the band width, and for a gaussian distribution gives the half-width at half-height by $\Delta E_{1/2} = (2 \ln 2)^{1/2}\Lambda_2^{1/2}$. The third moment Λ_3 is related to the band a symmetry (skewness), while Λ_4 yields the kurtosis, $(\Lambda_4/\Lambda_2^2) - 3$, which measures the intensity in the wings relative to that in a gaussian distribution.[9]

To illustrate these Λ_k's consider several simple examples. Suppose $F(E) = 1$ for $-1/2 \leq E \leq 1/2$, with $F(E) = 0$ otherwise. Then $\Lambda_k = \mu_k$, $\Lambda_2 = 1/12$, $\Lambda_4 = 1/80$, and $\Lambda_6 = 1/448$, with all odd $\Lambda_k = 0$. By contrast, a gaussian distribution $F(E) = (\alpha/\pi)^{1/2} \exp(-\alpha E^2)$, again with $\Lambda_k = \mu_k$ and all odd $\Lambda_k = 0$, yields $\Lambda_2 = (2\alpha)^{-1}$, $\Lambda_4 = (3/4\alpha^2)$, and $\Lambda_6 = (15/8\alpha^3)$. Here $\Lambda_4 = 3\Lambda_2^2$, while for the square distribution (first example) $\Lambda_4 = (9/5)\Lambda_2^2$, so that the latter has a negative kurtosis. A distribution with a positive kurtosis is $F(E) = (\alpha/2)\cdot \exp(-\alpha|E|)$, which yields $\Lambda_k = \mu_k = k!/\alpha^k$ for even k, $\Lambda_k = 0$ for odd k, and $\Lambda_4 = 6\Lambda_2^2$.

Odd moments are illustrated by the normalized right-triangular distribution $F(E) = 2(1 - E)$ for $0 \leq E \leq 1$, with $F(E) = 0$ otherwise. Here $\Lambda_k \neq \mu_k$ for $k > 1$, $\mu_k = 2/(k + 1)(k + 2)$, $\Lambda_1 = 1/3$, $\Lambda_2 = 1/18$, $\Lambda_3 = 1/135$, $\Lambda_4 = 1/135$, and $\Lambda_5 = 4/1701$, so that $\Lambda_4 = (12/5)\Lambda_2^2$.

A final detail of the method is that the partition functions Q needed for the Boltzmann populations are obtained by a summation over the finite number of vibrational eigenstates, the same as the number of basis functions. When both initial and final states are HO's with $b_2 = 1$ this is the only source of error, since the basis functions are eigenstates. At T = four units of $\hbar\beta/2$, Q for this case is calculated to be 2.54137, 2.54148, and 2.54148 with 20, 30, and 40 basis functions, respectively. Since the exact value is 2.54149, 30 functions are adequate for $T \leq 4$. For other potentials, including HO's that are displaced ($b_1 = 0$) or that have $b_2 = 1$, there is additional error due to the fact that eigenstates are not used, but instead a limited basis set approximation. Again by comparing results obtained with 20, 30, and 40 basis functions, we concluded that 30 functions were generally adequate for describing the states of most reasonable potentials provided that T is only a few energy units.[10]

(9) See, for example, R. von Mises, "Mathematical Theory of Probability and Statistics," Academic Press, New York, N. Y., 1964, pp 112–154.

Results

A. Variation in Force Constant

While a large variety of hypothetical potential curves can easily be considered with our method, it seemed desirable to concentrate on simple types having features in common with real molecules. Vibrations which induce electronic transitions change the symmetry of a molecule[11] and are frequently even functions of the displacement coordinate, thus eliminating all odd terms in eq 7. Examples would be the bend and antisymmetric stretch of a centrosymmetric linear triatomic. Thus these modes would not display the type of anharmonicity in the dissociative symmetric stretch, making the use of a short power-series expansion in eq 7 highly attractive. A reasonable model is the assumption of harmonic oscillators for both initial and final states. Considering first the case with no change in equilibrium geometry along the vibronically active coordinate, we present results in Figures 1–6 describing band shapes for vibronically induced transitions as a function of temperature and of the final-state force constant. In every case similar results for allowed transitions are added for comparison. The initial state HO has $b_2 = 1$ so that the basis states are its eigenstates, while the final state has one of the indicated b_2 values. The ratios of the final-state frequencies to the intial-state frequency are $2^{1/2}/2$, $3^{1/2}/2$, 1, $5^{1/2}/2$, and $6^{1/2}/2$ for $b_2 = 0.50$, 0.75, 1.00, 1.25, and 1.50, respectively. Temperatures (T)[12] are in energy units of $\hbar\beta/2$. The results in Figures 1–6 were all obtained using 30 HO basis functions for the expansions in eq 4.

Figure 1 displays computed spectral moments Λ_1, as defined by eq 11. In (a) we note that the thermal shift of the mean energy Λ_1 is considerably greater for the vibronically induced transition than for the allowed transition (b). Also in (a) the slope $d\Lambda_1/dT$ is nonvanishing at $T = 0$ for all b_2, with the sign of the slope changing from negative to positive at about $T = 1.5$ for $b_2 = 1.50$. Thus, when the final state has the higher vibrational frequency, the thermal shift of the mean energy changes from a red shift to a blue shift at some value of T. In the allowed case the slope $d\Lambda_1/dT$ approaches zero as T approaches zero for all b_2.

Figure 2 shows values of Λ_2 which are quadratic in energy. These results depend only on the magnitude of the change in force constant (related to b_2), but not on the sign, for the curves for $b_2 = 1.50$ and 0.50 are iden-

(10) For a discussion of choices of basis sets for one-dimensional potentials, see A. M. Lesk, *J. Chem. Phys.*, 49, 3898 (1968).

(11) More specifically it is the symmetry of the fixed-nuclei electronic Hamiltonian which is changed. Interestingly it is possible for totally symmetric vibrations to induce electronic transitions, provided that the electronic transition moment is very small at the initial-state equilibrium geometry but becomes significantly larger for moderate displacements.

(12) For molecules with light atoms T is less than one energy unit unless the temperature is significantly greater than room temperature, so that most of the following results for $T > 1$ will seldom be encountered in experimental spectra. However, for metal ions in crystals, striking thermal effects on intensities are observed at room temperature and below. A good example is the UCl_6^{2-} complex, where the vibronically active coordinate has a frequency of approximately 90 cm^{-1} so that T at room temperature is about four energy units: R. A. Satten and E. Y. Wong, *ibid.*, 43, 3025 (1965).

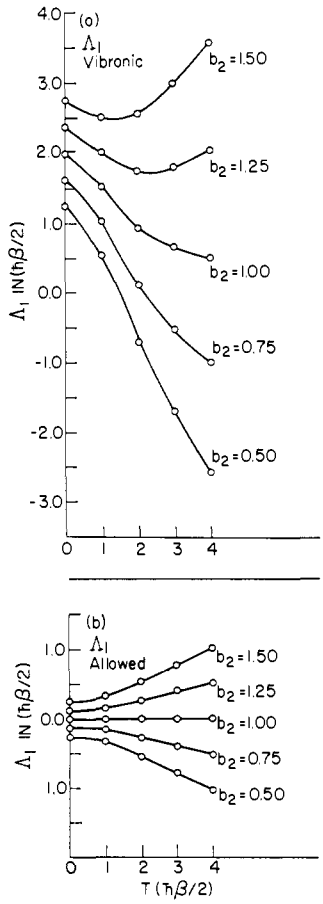

Figure 1. Spectral moments Λ_1 in units of $\hbar\beta/2$ *vs.* temperature in energy units $\hbar\beta/2$ for (a) a vibronically induced transition and (b) an allowed transition between harmonic oscillators (HO's) with differing force constants. In each case the initial state potential is given by $b_2 = 1.0$ (see eq 7), while the final state values of b_2 are the labels for the curves. Circled points here and in Figures 2–4 denote the calculated values.

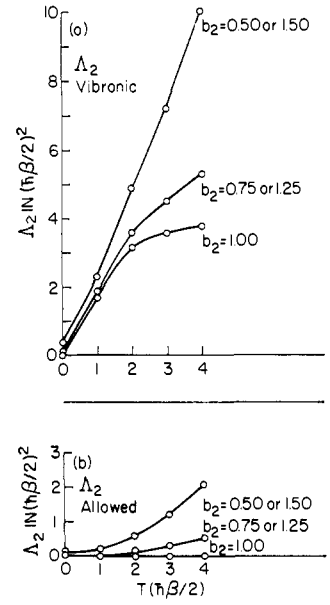

Figure 2. Plots of Λ_2 in units of $(\hbar\beta/2)^2$ *vs.* temperature for (a) a vibronically induced transition and (b) an allowed transition between HO's with differing force constants. See legend Figure 1.

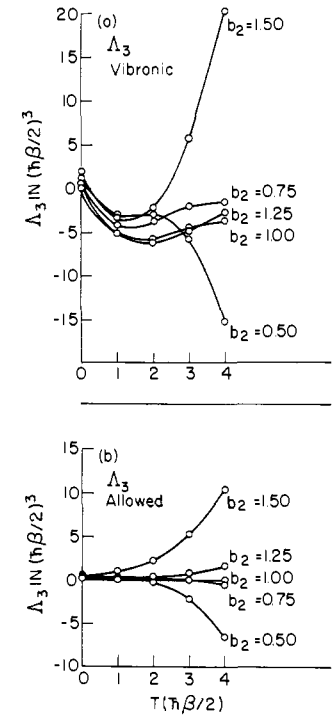

Figure 3. Plots of Λ_3 in units of $(\hbar\beta/2)^3$ *vs.* temperature for (a) a vibronically induced transition and (b) an allowed transition between HO's with differing force constants. See legend of Figure 1.

tical in both the vibronically induced and allowed cases. The linear variation in Λ_2 *vs.* T at small T in (a) indicates that the width of a vibronically induced band increases as $T^{1/2}$, a result pointed out[7] by Kubo and Toyosawa.

An interesting moment is Λ_3 (Figure 3), since it is a signed quantity. The differences between the vibronically induced and the allowed (b) cases do not appear to be great, except again for the nonvanishing of the slope in (a) for $T = 0$. It is interesting that the curves in (a) for $b_2 = 1.50$ and $b_2 = 0.50$ are nearly identical out to $T = 2$, where they begin to diverge very rapidly. This behavior is perhaps better illustrated by Figures 5 and 6, to be described later.

The moments Λ_5 and Λ_6 were computed but not plotted, while the Λ_4 is shown in Figure 4. The differences between the curves in (a) and those in (b) are mostly quantitative, the shapes being nearly identical. Even the quantitative differences are somewhat misleading, for Λ_4 is quartic in energy, exaggerating what would be small differences in the fourth roots which are linear in energy.

The spectral distributions represented by these moments are far from smooth, meaning that an accurate representation would require a very large number of moments. As an alternative method of display, Figures 5 and 6 show bar-graph idealizations of the same computed spectra. Here each ΔE interval of $\hbar\beta$ is assigned the intensity for any vibronically induced transition (solid lines) or allowed transition (dashed lines) whose energy falls within that ΔE interval. The initial-state spacings are also $\hbar\beta$, but the ΔE intervals are displaced by $\hbar\beta/2$, so that a $0 \rightarrow 1$ transition with no change in force constant occurs at two units of $\hbar\beta/2$, which is at the center of the bar that ranges from ΔE = one unit to ΔE = three units of $\hbar\beta/2$. If by chance ΔE equals the

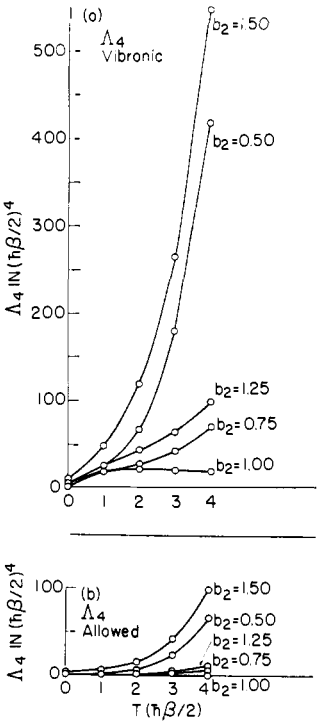

Figure 4. Plots of Λ_4 in units of $(\hbar\beta/2)^4$ *vs.* temperature for (a) a vibronically induced transition and (b) an allowed transition between HO's with differing force constants. See legend of Figure 1.

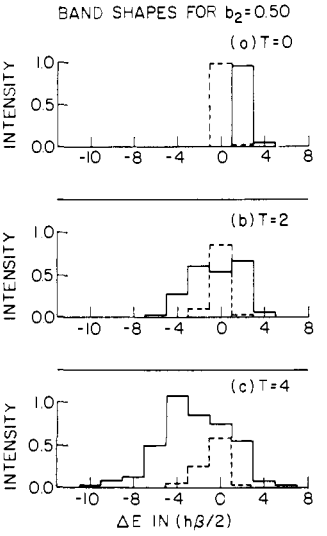

Figure 5. Bar graph representations of band shapes for vibronically induced transitions (solid lines) and allowed transitions (dashed lines) from an initial HO with b = 1.00 to a final HO with b_2 = 0.50, at temperatures of (a) 0, (b) 2, and (c) 4 energy units of $\hbar\beta/2$. The total band intensity, given by the sum of the heights of the bars, is unity in the allowed case, and coth $(1/T)$ in the vibronically induced case, where T is in energy units. Each ΔE interval of $\hbar\beta$ is assigned the intensity for any transition whose energy falls within that interval.

dividing value (any odd multiple of $\hbar\beta/2$), the corresponding intensity is arbitrarily assigned to the higher interval. In practice this situation has not arisen. Total band intensities are given by the sum of of the heights of the bars, this sum always being unity in the allowed case, but is coth $(1/T)$ in the vibronically induced case, satisfying eq 1, with T again in energy units

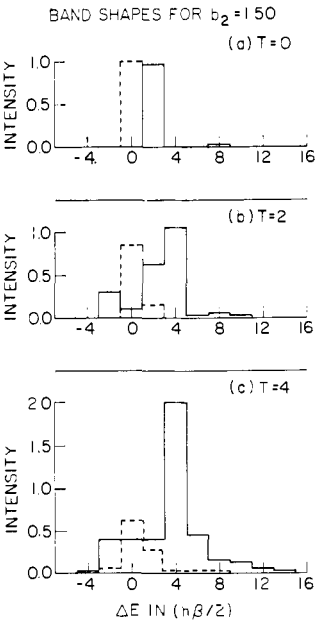

Figure 6. Bar graphs as in Figure 5, but for transitions from an initial HO with b_2 = 1.00 to a final HO with b_2 = 1.50, at temperatures of (a) 0, (b) 2, and (c) 4 energy units of $\hbar\beta/2$.

of $\hbar\beta/2$. Thus the vibronic intensity is 1.000, 2.164, and 4.083 at T = 0, 2, and 4, respectively. The actual sum of the f_{ij} of eq 2 is 0.5 at T = 0 for an HO with b_2 = 1, so all vibronically induced intensities have been doubled, yielding 1.0 in this case.

Figure 5 displays these results for b_2 = 0.50, meaning that the final-state force constant is less than the initial-state force constant. While there is in principle a distribution at T = 0 (a) of either the vibronically induced intensity (0 → 1, 0 → 3, 0 → 5, etc.) or the allowed intensity (0 → 0, 0 → 2, 0 → 4, etc.), nearly all of the intensity is in a single line even when the final b_2 is only one-half of the initial b_2. The greatly broadened distributions at T = 2 (b) and T = 4 (c) result primarily from the noncoincidence of the ΔE's for different v's of the transitions $\Delta v = \pm 1$ in the vibronically induced case or of the transitions Δv = 0 in the allowed case.

Figure 6 displays similar results but for b_2 = 1.50 (increase in force constant upon excitation). Here the vibronically induced distribution shifts toward the blue with rising T, in contrast to Figure 5, where the shift is to the red. Specifically, the vibronic intensity in the bar centered at ΔE = 2 at T = 0 is the 0 → 1 transition at 2.6742 units, while that in the bar centered at ΔE = 8 is the 0 → 3 transition at 7.5732 units. At T = 2 there appear the transitions 1 → 0 at −1.7752, centered at −2, 1 → 2 at 3.1238, centered at four units, plus numerous other weak transitions such as 1 → 4, 2 → 1, 2 → 3, 2 → 5, etc. One observation is that the asymmetries in the vibronically induced distributions at T = 2, Figures 5b and 6b, are not greatly different, so that the similarity in the Λ_3 values, Figure 3a, should not be surprising, especially since Λ_3 is defined relative to Λ_1. That is, Λ_3 is the mean-cube deviation from the mean. At T = 4, however, the asymmetries in Figures 5c and 6c appear qualitatively different, consistent with the previously noted divergence in Figure 3a for b_2 = 0.50 and 1.50.

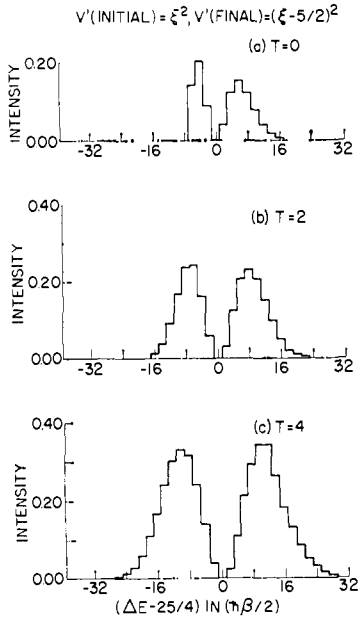

Figure 7. Bar graphs as in Figure 5, but for V' (initial) = ξ^2 and V' (final) = $(\xi - 5/2)^2$, so that V' (final) has $b_0 = 25/4$, $b_1 = -5$, and $b_2 = 1$. Only vibronically induced intensity is shown, at temperatures of (a) 0, (b) 2, and (c) 4 energy units of $\hbar\beta/2$. The energy scale is displaced (see text) by $25/4$ energy units.

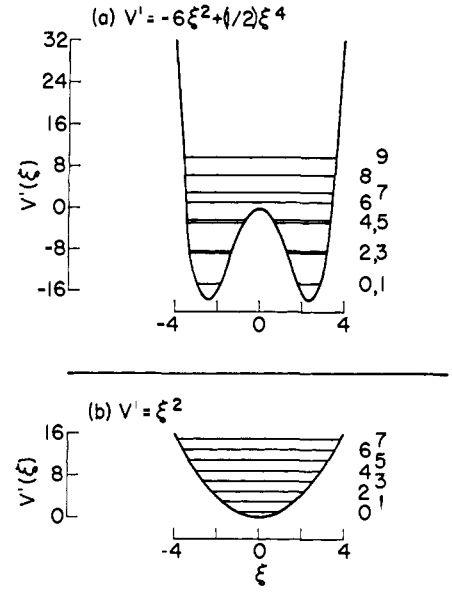

Figure 8. Potential energy curves and lowest few energy levels using 30 basis functions for (a) a double-minimum well and (b) a HO with $b_2 = 1$. The curves are a function of the dimensionless coordinate ξ as in eq 7, while the integers to the right of the curve are level indices v. In (a), the 0,1 separation is 0.00015, the 2,3 separation is 0.000731, and the 4,5 separation is 0.26344 energy unit, all levels with even or odd v corresponding to even or odd parity, respectively.

B. Variation in Equilibrium Geometry

While molecules will not usually have geometry changes along vibronically active coordinates, as opposed to other coordinates, such a situation is by no means impossible. Thus we calculated Λ_k values as a function of T for transitions between HO's with the same frequency ($b_2 = 1$ for both), but with different equilibrium positions. These positions are determined by the size of the coefficient b_1 in eq 7, with the minimum occurring, for $b_2 = 1$, at $\xi_0 = -b_1/2$, so that $V'(\xi_0) = 0$ if $b_0 = b_1^2/4$ is added to the potential. The vertical energy difference measured from one of the minima is also $b_1^2/4$ energy units. By comparison the ZPE is one energy unit, with a root-mean-square (rms) displacement of $\xi_{rms} = 2^{-1/2}$.

Calculations were made with $b_2 = 1$ for both initial and final states, but with the final state having $b_1 = -0.1$, -1.0, -5.0, or -10.0, and $b_0 = b_1^2/4$. The zero value of b_1 in the initial state is consistent with the assumption of an electronic transition moment proportional to x. We thus avoided introducing a constant term in the effective operator to compensate for an apparent origin dependence of the vibronic intensity, as occurs, for example, if the initial and final potentials had linear terms of $\pm b_1/2$, respectively. Results were obtained using either 20, 30, or 40 basis functions, although 30 functions appear to be adequate unless $|b_1|$ is greater than 5. For example, the interval between $v = 10$ and $v = 9$ is computed with 30 functions to be 2.00066 energy units when $b_1 = -5$, but 3.41245 units when $b_1 = -10$. In both cases the exact value is two units.

Figure 7 shows bar-graph representations of the vibronically induced spectra for $b_1 = -5$ with 30 basis functions. The energy scale is relative to the vertical energy difference of $25/4$ energy units at the initial state minimum. Since the transition is induced, there is no intensity in the vertical transition bar, for which ΔE equals $25/4$. By contrast, an allowed transition (not shown) has a usual Franck–Condon distribution, with a maximum in the vicinity of the vertical transition. The moments Λ_k for the vibronically induced case are not plotted but have the following characteristics: (a) Λ_1 shows a thermal red shift $\Delta\Lambda_1/\Delta T$ which is independent of b_1, and hence equal to that in Figure 1a for $b = 1.00$; (b) Λ_2 increases very rapidly with T only for small $|b_1|$, say <1; (c) Λ_3 exhibits a minimum at some $T \neq 0$ (Λ_3 for the corresponding allowed transition is independent of T and equal to b_1^2); and (d) Λ_4 is moderate in size, equaling about $3\Lambda_2^2$ or less.

A different example illustrating geometry change along a vibronically active coordinate is given by a HO initial state, shown in Figure 8b with its lowest few energy levels, and a final state having the potential in Figure 8a, also shown with its lowest few levels. The distribution of the vibronically induced intensity is shown in Figure 9, as obtained using 30 basis functions. The spectral moments (not shown) tend to be very large, with Λ_4 at T = four energy units equaling 9.201×10^7, which has a fourth root of 97.94 energy units. As the asymmetry in Figure 8 suggests, the third moment is positive, being 10.31, 1.126×10^3, and 2.023×10^5 at $T = 0$, 2, and 4 units, respectively.

An interesting situation occurs if the potentials of Figure 8 are reversed, taking the double-minimum curve for the initial state. While a vibronically induced spectrum can be calculated using a displacement coordinate measured from one of the minima at $\xi = \pm 6^{1/2}$, we assumed instead that the electronic transition moment was proportional to ξ (or x). Either way eq 1 is not satisfied, but more interesting the chosen way contains both allowed and vibronically induced character in terms of a coordinate measured from a minimum. The total intensity decreases slightly with rising temperature, with

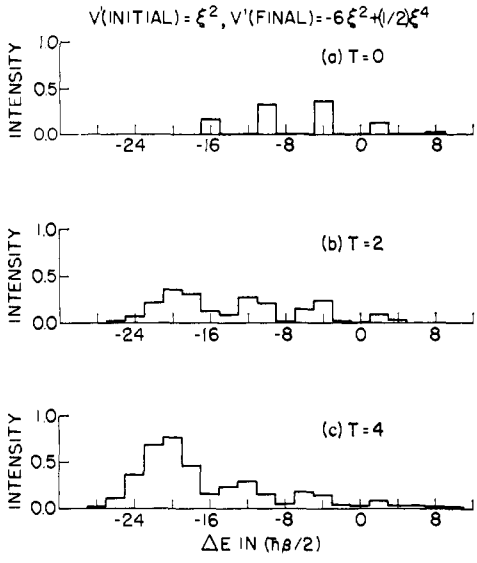

Figure 9. Bar graphs as in Figure 5, but for V' (initial) = ξ^2 and V' (final) = $-6\xi^2 + (1/2)\xi^4$. Only vibronically induced intensity is shown, at temperatures of (a) 0, (b) 2, and (c) 4 energy units of $\hbar\beta/2$.

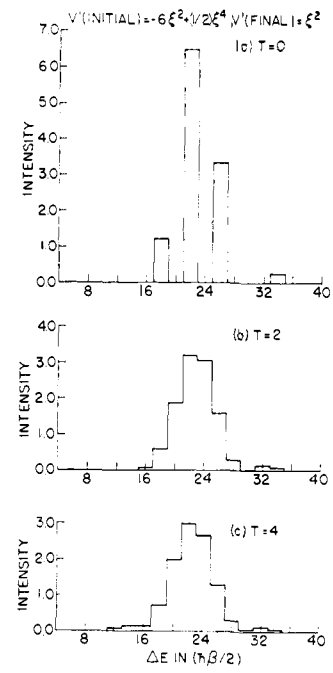

Figure 10. Bar graphs as in Figure 5, but for V' (initial) = $-6\xi^2 + (1/2)\xi^4$ and V' (final) = ξ^2. Only vibronically induced intensity is shown at temperatures of (a) 0, (b) 2, and (c) 4 energy units of $\hbar\beta/2$.

f = 11.390, 11.324, and 10.954 at T = 0, 2, and 4, respectively. The bar graphs in Figure 10 show that the distribution tends toward a Gaussian form with rising T, but that there remains considerable intensity in the wings at T = 4, where $\Lambda_4/\Lambda_2^2 = 1826.4/(14.64)^2 \approx 8.5$, significantly larger than the gaussian ratio of three. This example is, except for the lack of vibrational degeneracy, like an allowed transition from a bent state of a triatomic molecule to a state with a linear equilibrium structure, with the symmetry condition that the electronic transition moment vanishes for a linear configuration, so that the electronic moment varies with the bond angle. Figure 9 represents a forbidden transition from a linear state to a bent state, with the intensity induced by the bending vibration, again with its degeneracy ignored.

Summary

The intensity distributions associated with vibronically induced electronic transitions are found to differ from those for allowed transitions in several ways other than the familiar temperature dependence of the total intensity. For transitions between HO's with differing force constants, the spectral moments Λ_k and their temperature variation, particularly for k = 1, 2, and 3, may offer clues as to the presence of a vibronic intensity mechanism. If the equilibrium geometry changes along the vibronically active coordinate the distributions are particularly interesting. For a transition between HO's of the same frequency but different equilibrium position the distribution is characterized by two maxima, with an intensity minimum in the vicinity of the vertical energy difference, in sharp contrast to a Franck–Condon distribution. A transition from a HO to a double-minimum well displays a very broad asymmetric distribution, while a transition from a double-minimum well to a HO has a nearly gaussian distribution at large T. In this latter case the assumption of an electronic transition moment proportional to x implies an intensity with both allowed and induced character in terms of a coordinate x', measured from a minimum.

A difficulty in applying these results to experimental spectra is the complication of other vibrational modes along which there will be normal Franck–Condon distributions. The observed spectrum is a superposition of these distributions, with an energy scale which represents the total change in vibrational energy (plus an electronic energy as a trace). In a future communication we plan to present theoretical distributions which have been summed over all the modes present in small polyatomic molecules. While the observation of two maxima in a spectrum is usually interpreted as evidence for two separate electronic transitions, our results suggest the possible alternative of a single vibronically induced transition with a change in equilibrium geometry along the vibronically active coordinate.

Acknowledgments. The author wishes to thank the University of Michigan for a Du Pont summer research grant. He also thanks Dr. Walter G. Rothschild for suggesting the use of harmonic oscillator basis functions and for providing a portion of the necessary computer program.